Influence of Additives on the Thermoresponsive Behavior of Polymers in Aqueous Solution

Kurt Van Durme, Hubert Rahier, and Bruno Van Mele*

Department of Physical Chemistry and Polymer Science, Vrije Universiteit Brussel, Brussels, Belgium

Received August 17, 2005; Revised Manuscript Received September 30, 2005

ABSTRACT: The effect of additives on the LCST phase behavior of aqueous solutions of either poly(*N*-isopropylacrylamide) (PNIPAM) or poly(vinyl methyl ether) (PVME) has been investigated using high-resolution ultrasonic spectroscopy (HR-US) and modulated temperature differential scanning calorimetry (MTDSC). Both techniques revealed that the addition of salt causes a decrease in demixing temperature (T_{demix}) due to the water-structuring capacity of salt ions. This salting-out effect becomes more pronounced at high polymer concentration, causing an asymmetric shape of the LCST demixing curve. Conversely, adding a surfactant results in an increase of T_{demix} because of the increased solubilization of the polymer chains. In addition, HR-US provides supplementary information on a molecular level, illustrating that both types of additives dissimilarly affect the polymer−water hydration structure; i.e., salt ions primarily dislocate the structured water molecules, whereas surfactants interact with the polymer itself.

Introduction

Intelligent water-soluble polymers have attracted considerable interest as they often display large, reversible conformational changes in response to small external stimuli, causing a change in physical or chemical properties.[1] Among this class of materials, thermoresponsive polymers have been extensively studied as they can serve as simple analogues to mimic the water solubility of, for instance, proteins and other biopolymers.[2] Such aqueous polymer systems are frequently characterized by a lower critical solution temperature (LCST) type of demixing behavior, which implies that the polymers dissolve (swell) in water at low temperature. Increasing the temperature causes the polymer to phase separate from the aqueous solution whereas the cross-linked analogues may display an order-of-magnitude change in hydrogel size. Therefore, such materials can be used in numerous applications as actuators,[3,4] artificial muscles,[5] dewatering membranes,[6] drug delivery systems,[7−10] thermoresponsive surfaces,[11−13] light modulation systems,[14] and molecular recognition agents.[15,16] The temperature-induced phase separation process in aqueous polymer systems originates from varying inter- and intramolecular interactions upon heating.[17,18] At low temperature the homogeneous mixture exhibits predominantly intermolecular hydrogen bonding as demonstrated by various experimental techniques.[19−22] Heating the polymer/water mixture promotes hydrophobic interactions between the polymer chains, causing aggregate formation accompanied by an endothermic heat effect and an intensifying opacity of the originally transparent solution.[23−32]

In terms of thermodynamics, the liquid−liquid phase behavior of a polymer mixture is usually explained using the Flory−Huggins lattice theory, taking into account specific interactions. To describe the different types of phase separation that have been experimentally observed, the interaction function needed to be regularly adjusted. In this respect, Šolc et al. introduced an extensive concentration dependence[33] that later on turned out to be at least a cubic polynomial function to get an acceptable fit of the data for aqueous polymer systems.[34,35] Once this function is known, the entire phase diagram can be calculated, by minimizing the Gibbs free energy of mixing for any given composition. The polynomial expression of the modified interaction function will generate additional roots, but only three are meaningful. The first possibility leads to the classical Flory−Huggins demixing behavior with a critical concentration that shifts toward the solvent axis and lower temperature as the polymer chain length increases. Such behavior is also called type I and was, for instance, observed for the poly(*N*-vinylcaprolactam) (PVCL)/water system.[26,27]

One extra root is responsible for what is called type II demixing behavior, which includes a critical point independent of the polymer chain length at off-zero concentration, found for the poly(*N*-isopropylacrylamide) (PNIPAM)/water system.[28−30] Finally, two extra roots lead to the so-called type III demixing behavior, characterized by a bimodal demixing curve, typically observed for the poly(vinyl methyl ether) (PVME)/water system.[25,31−34] In this case, three different two-phase areas can be distinguished (often referred to as α, β, and γ). The critical point at low polymer concentration again represents the classical Flory−Huggins demixing behavior (α-domain), while the β-domain displays type II demixing behavior. Both areas are separated from the γ-domain by an invariant three-liquid-phase coexistence line at constant temperature.

Other theoretical approaches are available, but most of them address the problem of, for instance, bimodality in a semiempirical way; i.e., extra terms are added to ascertain a sufficiently pronounced concentration dependence of the interaction function used, which makes the description of multiple critical points feasible.[36−40]

The above-mentioned descriptions assume the polymer to be monodisperse so that the polymer solution can be treated as a strictly binary system. Synthetic polymers, however, are always polydisperse and should therefore be treated as quasi-binary systems, which makes its theoretical description less straightforward. Hence, in the quasi-binary treatment coexistence curves

* Corresponding author: Fax +32-(0)26293278; Ph +32-(0)-26293288; e-mail bvmele@vub.ac.be.

10.1021/ma051816t CCC: $30.25
Published on Web 11/03/2005

Table 1. Hofmeister Series According to Ref 59

	strongly hydrated							weakly hydrated
anions	SO_4^{2-}	> HPO_4^{2-}	> F^-	> Cl^-	> Br^-	> I^-	> NO_3^-	> ClO_4^-
cations	Al^{3+}	> Mg^{2+}	> Ca^{2+}	> H^+	> Na^+	> K^+	> Rb^+	> Cs^+ > NH_4^+

become cloud point curves, the invariant three-phase line at constant temperature becomes a three-phase region, etc. Similar adaptations hold for multicomponent (e.g., ternary) systems, causing the information on this topic to be less available.[41−43] More details on strictly binary, quasi-binary, and ternary systems can be found elsewhere.[44]

These phenomenological (and thermodynamically correct) approaches, describing the different types of LCST miscibility behavior (I, II, and III), cannot explain the observed differences on a molecular level. Therefore, Nies et al. recently started to adapt the general theory of Wertheim for saturation interactions[45] to the lattice model, especially focusing on the phase behavior of polymer solutions. With this approach, the hydration concept can be theoretically quantified on the basis of the balance of dispersive and saturation interactions between the solvent and the polymer under investigation. In this way, the bimodal LCST miscibility gap (at physiological temperatures) of the PVME/water system could be predicted and understood on a molecular basis, together with other liquid−liquid and solid−liquid coexistence data at subzero temperatures.[46−48] This new approach allows explaining the thermodynamic behavior of different polymer mixtures as a function of pressure, temperature, composition, and chain length in terms of the relevant molecular interactions between polymer and solvent. The effect of additives might be explained similarly by introducing additional molecular interactions. However, the theoretical extension, from a (quasi)-binary to a ternary system in the presence of additives, is beyond the scope of the current paper, which aims at a thorough experimental description of the role of additives in aqueous polymer systems using high-resolution ultrasonic spectroscopy (HR-US) and modulated temperature differential scanning calorimetry (MTDSC) as innovative analytical techniques.

The thermoresponsive behavior of polymers in aqueous solution can easily be varied by addition of small molecules, as these in general alter the polymer−water interactions. Salts, for instance, are known to disrupt the hydration structure surrounding the polymer chains, causing a decrease in demixing temperature.[49−58] This alteration is ion-dependent, which can be represented by the well-known Hofmeister series (Table 1)[59] which originates from the ability of ions to precipitate egg white proteins, for both anions and cations. The most destabilizing ions are known as structure-makers or kosmotropes, while the more stabilizing ones are called structure-breakers or chaotropes. Alternatively, the ability of additives for binding water molecules can also be expressed by the Jones-Dole viscosity B coefficient, reflecting the change in viscosity regarding pure water.[60,61]

Surfactants, contrary to salts, are often used to obtain a stable aqueous dispersion of hydrophobic solutes.[62] By doing so, the properties of both the solute and the surfactant are mutually modified, which was already thoroughly elaborated for dilute polymer solutions.[63−67] Several studies revealed that the surfactant molecules adsorb onto the polymer by means of their hydrophobic tails, either individually or in micellar form.[68−71] Hence, the addition of surfactants causes an improved solubilization of the polymer chains, usually reflected by elevating the phase separation temperature.[72−75] Increasing the surfactant concentration may well inhibit aggregation of the collapsed polymers or even prevent the coil-to-globule transition entirely.[76−79] This will be decided by the polymer conformation and the amount of repulsive electrostatic interactions between the ionic heads of the adsorbed surfactant molecules, which depend on the nature of the surfactant and polymer used. That is why, in contrast to salts, it is less straightforward to generalize the potential consequences of adding surfactants on the phase separation properties of polymer/water mixtures.

In this work we will investigate the influence of both salts and surfactants on the water solubility of PNIPAM (type II LCST) and PVME (type III LCST) for mixtures spanning the entire composition range, in contrast to literature where such evaluation is usually limited to dilute polymer solutions. In this respect recently introduced high-resolution ultrasonic spectroscopy (HR-US) will be applied together with MTDSC. The former technique is based on measuring the resonance characteristics of ultrasonic waves propagating through a sample. The produced oscillating pressure causes mechanical deformation of the studied material; i.e., compression in the ultrasonic wave changes the intermolecular distances in the sample, to which the molecules respond by intermolecular repulsions, causing them to return to their original positions. The propagation of a sound wave thus depends on the transfer of vibrations from one molecule to another. Therefore, ultrasonic spectroscopy enables direct probing of the intermolecular forces in the analyzed medium and thus the analysis of its physical and chemical properties.[80−84] The propagation of ultrasonic waves is essentially described by its velocity and attenuation. The ultrasonic velocity is extremely sensitive to intermolecular interactions, molecular organization, and composition of the analyzed medium, since these properties induce variations in the sample compressibility, which is the main factor determining the ultrasonic velocity.[81−86] The ultrasonic attenuation results from energy losses during consecutive compressions and decompressions while the ultrasonic wave goes through the sample. In nonhomogeneous samples (e.g., phase-separated mixtures), these energy losses contain a large contribution originating from the scattering of ultrasonic waves, making HR-US an appropriate technique to evaluate aggregate formation.[81,83,84] The calculation of the ultrasonic parameters (i.e., velocity and attenuation) along with a more profound discussion on the principles of the HR-US technique itself can be found in the literature.[80,83]

In this paper the results from HR-US will be used to support observations made by optical microscopy (OM) and MTDSC, which already proved to be a powerful tool for characterizing demixing and remixing in polymer solutions.[25,27,29,30,32]

Experimental Section

Materials. PNIPAM was obtained from PolySciences Inc., having a weight-average molecular weight (M_w) of 74 000 g mol^{-1}, whereas PVME (dissolved in water, 50/50 w/w) was purchased from Aldrich Chemical Co. Inc. (M_w = 20 000 g mol^{-1}). The polymers were dried under vacuum for at least 48 h at 130 or 40 °C, respectively, until the water content was less than 0.2 wt % as determined by thermogravimetric analysis (TA Instruments TGA 2950). The glass transition

temperature of dried PNIPAM is 140 °C, while that of PVME equals −25 °C.

Salt-containing aqueous solutions were obtained by adding NaCl, $CaCl_2$, or Na_2SO_4 to demineralized water, having concentrations of either 0.173, 0.349, or 0.524 M, whereas surfactant-containing aqueous solutions (0.035 M) were obtained by introducing sodium dodecyl sulfate (SDS). Henceforth, a range of polymer/solvent compositions (w/w) was prepared, by adding the appropriate amount of water (with or without additives) to the dry polymer. These mixtures were initially stirred at room temperature, after which they were stored at 4 °C for at least 2 weeks to promote homogenization.

Characterization. *Optical Microscopy (OM).* Cloud points were determined by measuring the light transmitted through thin samples between glass slides mounted in a Mettler Toledo FP82HT hot stage, which was placed in a Spectratech optical microscope (magnification ×10) equipped with a photodetector (most sensitive at a wavelength of 615 nm). Temperature calibration was done with benzophenone. Nonisothermal experiments were performed at 0.5 °C min^{-1}, using a nitrogen purge to cool below room temperature. A threshold value of 2% in the decrease of light transmittance (against 100% for the transparent homogeneous solution) upon heating was chosen as the cloud point temperature.

Modulated Temperature Differential Scanning Calorimetry (MTDSC). MTDSC measurements were performed on a TA Instruments 2920 DSC with the MDSC option and a refrigerated cooling system (RCS). Helium was used as a purge gas (25 mL min^{-1}). Indium and cyclohexane were used for temperature calibration. The former was also used for enthalpy calibration. Heat capacity calibration was performed with water at 20 °C. Data are expressed as specific heat capacities (or changes) in J g^{-1} K^{-1}. Standard modulation conditions were an amplitude of 0.50 °C with a period of 60 s. Nonisothermal experiments were performed at an underlying heating/cooling rate of 0.2 °C min^{-1}. Samples of 1−5 mg were introduced in Mettler aluminum pans that are subsequently hermetically sealed.

High-Resolution Ultrasonic Spectroscopy (HR-US). High-resolution ultrasonic spectroscopy measurements were performed on an Ultrasonic Scientific HR-US 102 spectrometer fitted with two 1 mL cells. The principles of the measurement of ultrasonic velocity and attenuation, employed in this method, are described earlier.[80] All experiments were done at selected frequencies: 7.5, 11.6, and 14.6 MHz. The cells were filled with 1 mL of water (reference) and polymer/solvent, respectively. Temperature control was achieved by using a Julabo HD-4 water bath. Standard heating/cooling rates were 0.2 °C min^{-1}. The polymer solutions in the HR-US cell were not stirred to have similar experimental conditions as in the other analytical techniques, unless mentioned otherwise.

Results and Discussion

The phase separation properties of polymers in aqueous solution are easily affected by the presence of small molecules (e.g., salts, surfactants, alcohols, etc.) as these alter the polymer−water interactions. In this section, the perturbation strength of several additives will be investigated using MTDSC, HR-US, and OM. This examination will be performed for compositions spanning the entire concentration interval in order to construct a state diagram.

Influence of Salt on the Phase Behavior of PNIPAM/Water. Salts are known to influence the phase behavior of aqueous PNIPAM solutions, since they disrupt the hydration structure surrounding the polymer chains. Sodium chloride (NaCl) is a typical example of what is called a water structure-maker, which implies that the hydration sheath near the polymer chains becomes partially destroyed. This explains why the addition of NaCl decreases the demixing temperature of the aqueous polymer solution upon heating,[56,57] as illustrated in Figure 1 for a 5/95 PNIPAM/water mixture using OM. The initial decrease in (normalized) light transmittance is used to define the cloud point temperature, which results from the aggregation of collapsed polymer chains during the phase separation process.[17,24,87] This hydrophobic association in conjunction with the intermolecular breaking of hydrogen bonds causes an endothermic heat effect, which can be studied using MTDSC. By doing so, the total demixing enthalpy is separated into two endothermic contributions, of which the largest part is found in the heat capacity signal (and as such in the reversing heat flow), whereas the nonreversing heat flow contains the other part.[29,30] Hence, the former signal is termed apparent (c_p^{app}) to distinguish it from the baseline specific heat capacity, c_p^{base}. Figure 2 shows the evolution of c_p^{app} upon heating a 30/70 PNIPAM/water solution with various amounts of NaCl. The initial deviation of c_p^{app} from the extrapolated experimental c_p^{base} (Figure 2, dashed line) indicates the start of phase separation, which is found at lower temperature as salt is added to the aqueous polymer mixture.

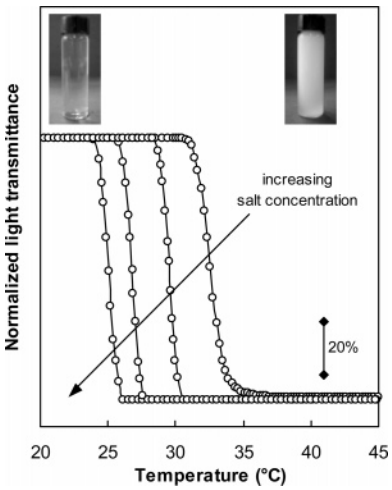

Figure 1. Normalized light transmittance during nonisothermal demixing of 5/95 PNIPAM/water with varying amounts of NaCl: 0, 0.173, 0.349, and 0.524 M.

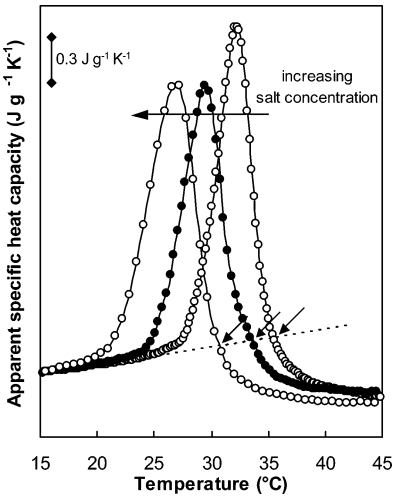

Figure 2. c_p^{app} during nonisothermal demixing of 30/70 PNIPAM/water with varying amounts of NaCl: 0, 0.173, and 0.349 M. Dashed line (extrapolated experimental c_p^{base}) is a guide to the eye. Tilted arrows indicate drop of c_p^{app} below c_p^{base} (considered as onset of partial vitrification).

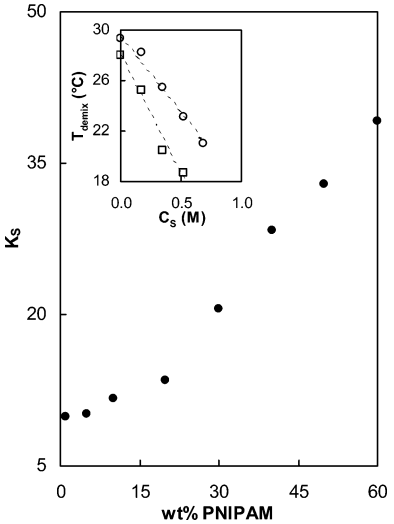

Figure 3. Concentration dependence of K_s for PNIPAM/water with 0.173 M NaCl, according to eq 1. Inset: T_{demix} vs molar salt concentration for a 10/90 (○) and a 30/70 (□) PNIPAM/water mixture.

Both Figure 1 and Figure 2 clearly illustrate that the depression of the phase separation temperature enlarges as the salt concentration increases (indicated by the arrow).[54,57] This can be represented by following linear relationship (see also Figure 3, inset):[51]

$$T_{\mathrm{demix}} = T^0_{\mathrm{demix}} - K_S C_S \qquad (1)$$

with T_{demix} and T^0_{demix} the demixing temperatures in the presence and absence of salt, respectively, and C_S the molar salt concentration. K_S is a measure of the salt effectiveness in modifying the stability of the aqueous polymer solution. This empirical factor K_S becomes larger as the polymer concentration increases (Figure 3), which can be understood by considering the Frank-Wen model.[50] The available water molecules will primarily hydrate the added ions, by which fewer water molecules are able to contribute to the polymer hydration sheath. Consequently, the salting-out effect is best noticeable at high polymer concentration (Figure 3). As a result, the demixing temperature of concentrated PNIPAM/water mixtures decreases to a larger extent, which is reflected in the variation of the (type II) LCST demixing curve (Figure 4a).

The change in polymer hydration sheath will also affect the glass transition temperature (T_g) of the homogeneous aqueous polymer mixture since the accessible water molecules plasticize the nearby polymer chains. Therefore, the addition of salt, which involves partial dehydration of the polymer, inevitably results in a higher T_g value and thus in an elevation of the T_g−composition curve (Figure 4b, compare + with × for the binary and ternary mixture, respectively). This increase in glass transition temperature again becomes more pronounced as the molar salt concentration increases, although in a nonlinear manner unlike T_{demix} (Figure 3). The T_g of, for instance, a homogeneous 90/10 PNIPAM/water mixture increases from 43 °C (no salt) to 52 °C (C_S = 0.173 M NaCl) or to 68 °C (C_S = 0.349 M NaCl), depending on the amount of NaCl added. The higher T_g value proves that there are fewer water molecules surrounding the polymer chains, thus indicating that the structuring capacity of salt is larger than that of the polymer. This seems to agree with earlier

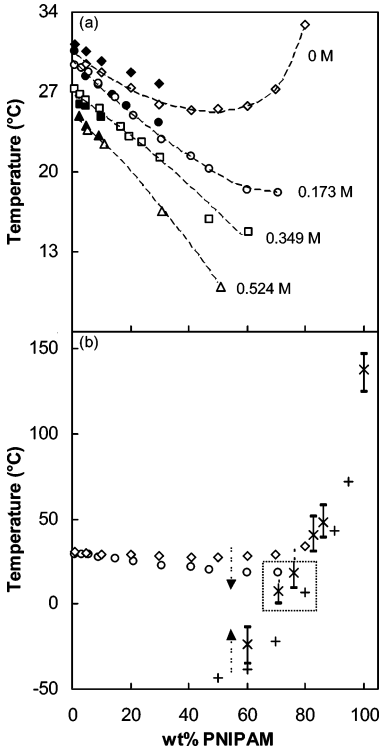

Figure 4. State diagram of PNIPAM/water with varying amounts of NaCl: (a) demixing curves with MTDSC (◇, ○, □, △) and OM (◆, ●, ■, ▲); dashed lines are a guide to the eye; (b) demixing curves for 0 M (◇) and 0.173 M (○), and T_g−composition curve for 0 M (+) and 0.173 M (×, width ΔT_g: I), all determined with MTDSC. Square indicates intersection LCST demixing curve with T_g−composition curve for 0.173 M NaCl.

studies, in which most authors state that the available ions exert their influence almost exclusively via their water-structuring capability and less (or not) via direct interactions between ions and monomeric units.[50−52,88,89]

In previous work we demonstrated that further heating of either aqueous PNIPAM solutions[29,30,83] or hydrogels[30] induces partial vitrification of the formed PNIPAM-rich phase, which can be seen as a drop in c_p^{app} below c_p^{base} (indicated by the tilted arrows in Figure 2) near that temperature at which the LCST demixing curve intersects with the T_g−composition curve. Hence, combination of the lower LCST demixing curve together with the higher position of the T_g−composition curve (depending on the amount of salt added) causes the vitrification of the PNIPAM-rich phase during phase separation to occur at both lower temperature and lower PNIPAM concentration (indicated by the square in Figure 4b). The former observation (i.e., lower temperature) is nicely illustrated in Figure 2, since the drop in c_p^{app} below c_p^{base} (Figure 2, dashed line) happens at lower temperature as the molar salt concentration increases. At much higher temperatures, near the glass transition temperature of the polymer-rich phase (ca. 140 °C), c_p^{app} again increases toward the extrapolated experimental c_p^{base} (not shown). The second observation (i.e., lower PNIPAM concentration), on the other hand, explains why each demixing curve from Figure 4 ends at a different polymer concentration; i.e., no phase separation can be observed for those mixtures having an amount of PNIPAM exceeding the PNIPAM/water composition at which the LCST demixing curve meets the T_g−composition curve. These structural changes within the sample cannot be observed using OM since

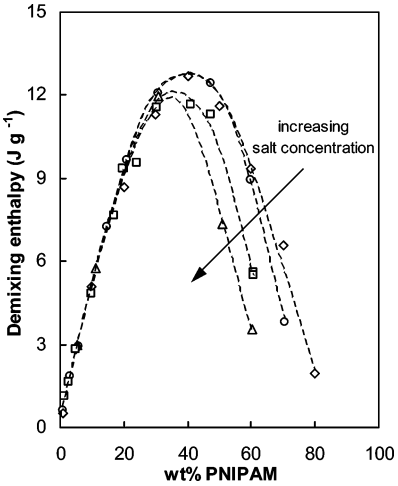

Figure 5. Demixing enthalpy (per gram of solution) as a function of concentration for PNIPAM/water with varying amounts of NaCl: 0 M (◇), 0.173 M (○), 0.349 M (□), and 0.524 M (△). Dashed lines are a guide to the eye.

the (normalized) light transmittance immediately drops to zero at the cloud point temperature. The shift in both T_{demix} and T_g will determine the shape of the demixing endotherm, which in general becomes wider when salt is added (Figure 2), in agreement with the enlarged temperature interval wherein compositional changes must occur according to the LCST demixing curve (Figure 4).[53,57]

Integration of the endothermic heat effect (by extrapolating the baseline of the total heat flow signal) yields the demixing enthalpy, which is mainly governed by the destruction of hydrogen bonds between the polymer and the surrounding water molecules. This composition-dependent heat effect hardly depends on the amount of NaCl added, when evaluating less concentrated mixtures, i.e., ≤30 wt % PNIPAM (Figure 5). However, at higher polymer concentration the observed endothermicity rapidly diminishes, since in that region the added salt displays the largest perturbation strength.

The superior water-structuring capability of salt, which was already elucidated via the increase in glass transition temperature, can also be investigated using HR-US, since the compressibility difference between bound and free water causes a dramatic change in the ultrasonic velocity value.[83,84,90] Figure 6a shows the evolution of the difference ultrasonic velocity upon heating a 5/95 PNIPAM/water mixture in the presence (upper curve) and absence (lower curve) of salt. Note that in order to analyze the details of the transition, the contribution of pure water was subtracted, and the difference in velocity is used instead of the absolute value. This kind of evaluation has already been extensively elaborated in previous work.[83,84] Figure 6a clearly illustrates that the (difference) ultrasonic velocity value substantially increases upon adding salt, which points to a larger amount of bound water in the ternary mixture, consequently illustrating the superior water-structuring capacity of salt (within the entire temperature interval). Furthermore, a nearly stepwise change at a certain temperature is noticed, caused by the phase separation process that reflects the variation in the hydration structure around the polymer chains and in the compressibility of the formed polymer aggregates. Indeed, below the demixing temperature the molecular structure of PNIPAM in water exhibits predominantly

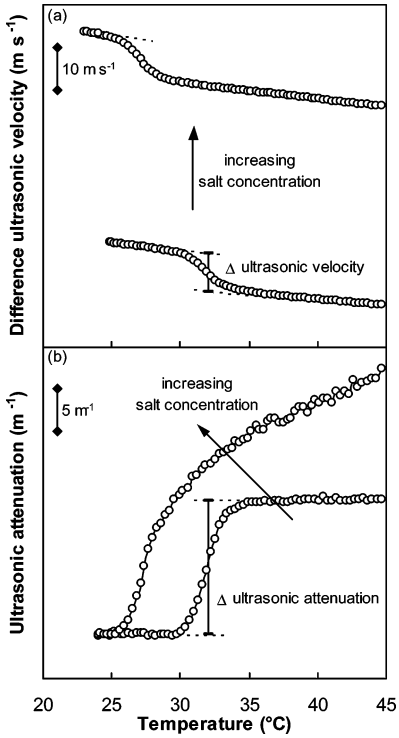

Figure 6. Difference ultrasonic velocity (a) and ultrasonic attenuation (b) during nonisothermal demixing of 5/95 PNIPAM/water with varying amounts of NaCl: 0 and 0.349 M. Lines are a guide to the eye.

intermolecular hydrogen bonding (amide−water), while above T_{demix} the intrachain hydrogen bonding (amide−amide) and hydrophobic interactions dominate. As a result, the amount of free water will considerably augment during the demixing process, which causes a significant decrease in the ultrasonic velocity since free water is typically more compressible than bound water.[90] Figure 6a again demonstrates that the addition of NaCl lowers T_{demix}, in agreement with the previously discussed results from OM (Figure 1) and MTDSC (Figure 2).

The ultrasonic attenuation signal (Figure 6b) that is related to the scattering of ultrasonic waves within the sample reflects the ongoing morphology changes during phase separation.[83−85] Below T_{demix} a rather constant attenuation level is generally observed, which is representative for the (entangled) polymer coils in the aqueous solution. This ultrasonic attenuation value of the homogeneous mixture is hardly influenced by the presence of salt. Once demixing sets in the attenuation sharply increases due to the scattering of ultrasonic waves that results from the aggregation of the collapsed PNIPAM chains. At somewhat higher temperature the attenuation tends to level off, which coincides with the onset of partial vitrification of the PNIPAM-rich phase during phase separation, in agreement with the temperature at which c_p^{app} drops below c_p^{base} when using MTDSC (Figure 2). Note that the leveling off gets less pronounced for the salt-containing mixture due to a higher degree of aggregation (see later). Nonetheless, the evolution with temperature of both the ultrasonic velocity and attenuation reflects the ongoing compositional changes governed by the PNIPAM/water state diagram (Figure 4b).

On the basis of Figure 6, the almost stepwise change in both velocity and attenuation can be evaluated. These stepwise changes (Δ), denoted as Δ ultrasonic velocity

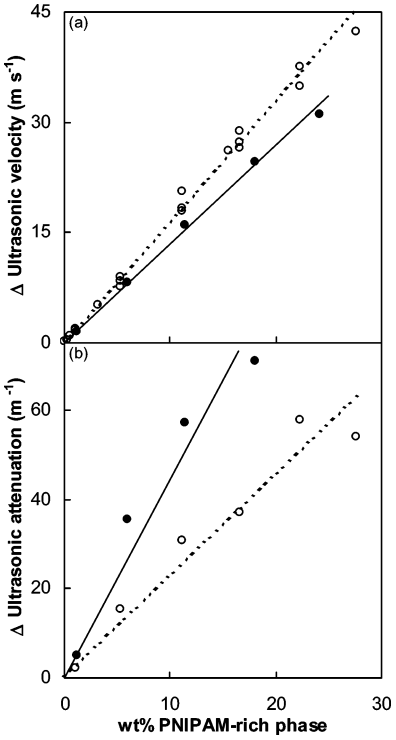

Figure 7. Concentration dependence of variation of ultrasonic properties (near T_{demix}) for PNIPAM/water with varying amounts of NaCl: 0 M (○) and 0.173 M (●).

and Δ ultrasonic attenuation, are to a large extent due to the formed PNIPAM-rich phase, illustrating the compositional changes in the sample that occur between T_{demix} and the temperature at which the LCST demixing curve intersects with the T_g−composition curve. Δ ultrasonic velocity is related to the change in compressibility caused by the release of water molecules previously surrounding the polymer chains, while Δ ultrasonic attenuation is related to energy losses caused by aggregation. The more and/or the larger the aggregates formed, the larger the stepwise changes expected. This is confirmed in Figure 7 since both quantities show an almost linear evolution with the fraction of the PNIPAM-rich phase formed (lever rule applied on the LCST curve of Figure 4b, starting from a homogeneous solution). The addition of salt considerably reduces the amount of structured water layers adjacent to the polymer chains, which accordingly causes a smaller (stepwise) change in the (difference) ultrasonic velocity and a larger increase in the ultrasonic attenuation as hydrophobic associations are promoted (Figure 7, compare ○ with ●). Note that, once vitrification occurs, the PNIPAM-rich phase is determined by the T_g−composition curve (and no longer by the LCST demixing curve), which generates smaller compositional changes and consequently less variation in the ultrasonic parameters (not included in Figure 7).

To verify the effect of different anions and cations on the demixing properties of aqueous polymer solutions, other ternary mixtures were investigated. Figure 8 shows that changing the cation ($Na^+ \rightarrow Ca^{2+}$) hardly influences the variation in phase separation temperature, while changing the anion ($Cl^- \rightarrow SO_4^{2-}$) induces a much larger decrease of T_{demix}. These observations are in nice agreement with the ion positioning in the Hofmeister series (Table 1).[59]

Influence of Salt on the Phase Behavior of PVME/Water. We also studied the influence of salt on

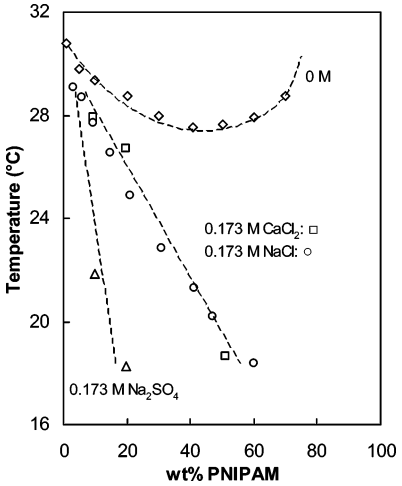

Figure 8. State diagram of PNIPAM/water with different salts: demixing curve from MTDSC for 0 M (◇) and 0.173 M (○) NaCl, 0.173 M $CaCl_2$ (□), and 0.173 M Na_2SO_4 (△). Dashed lines are a guide to the eye.

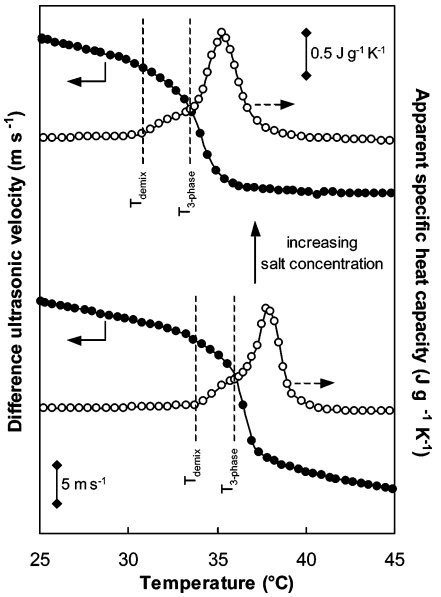

Figure 9. Nonisothermal demixing of 5/95 PVME/water with varying amounts of NaCl (0 and 0.173 M): difference ultrasonic velocity (●) and c_p^{app} (○, curves are shifted vertically for clarity).

the water solubility of PVME (Figure 9) for which, unlike PNIPAM, vitrification does not interfere with the phase separation process because the T_g−composition curve is situated well below the LCST demixing curve. Moreover, the PVME/water system shows a bimodal (type III) LCST partial miscibility behavior (Figure 10a, ◇), which consists of two lower two-phase areas separated from one upper two-phase area by a three-liquid-phase coexistence line at constant temperature.[31,32,34,35,84] Consequently, the PVME/water system displays two stable liquid−liquid critical points: one which obeys the classical Flory−Huggins theory, i.e., it decreases with increasing polymer molar mass and a second one (at high PVME concentration), which is nearly molar mass independent. Accordingly, the demixing process of PVME/water consists of two distinct steps,[31,32,84] as can be observed by HR-US and MTDSC, indicated by the vertical lines in Figure 9. That is to say, the initial stages of phase separation, above T_{demix}, are followed by large compositional changes upon passing the tem-

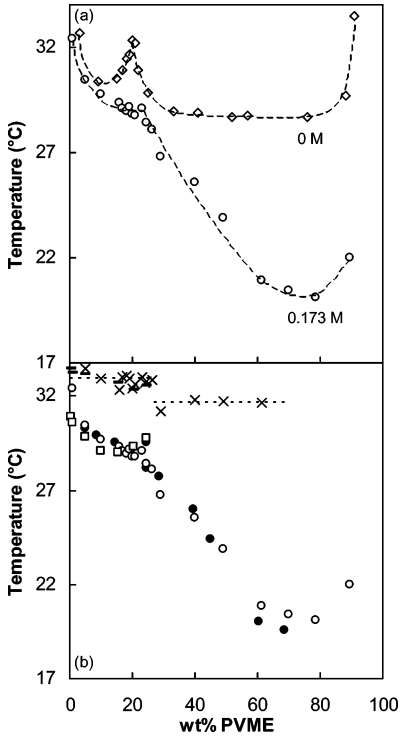

Figure 10. Demixing curves of PVME/water with varying amounts of NaCl: (a) with MTDSC (◇, ○); (b) with MTDSC (○), OM (●) and HR-US (□), together with $T_{3-\text{phase}}$ from MTDSC (×) and HR-US (—). Dashed lines are a guide to the eye.

perature at the three-phase equilibrium ($T_{3-\text{phase}}$). This two-step process cannot be seen using OM, since the normalized light transmittance immediately drops to zero at T_{demix} when studying nondilute mixtures (≥3 wt % PVME). This is caused by the level of aggregation, making it impossible to detect additional structural changes (e.g., $T_{3-\text{phase}}$).

Figure 9 also illustrates that the addition of NaCl lowers the demixing temperature. Moreover, the observed transition region in both the difference ultrasonic velocity (HR-US, ●) and the apparent specific heat capacity (MTDSC, ○) becomes wider, indicating that the temperature interval in which compositional changes occur enlarges. This observation corresponds to the more asymmetric shape of the bimodal LCST demixing curve, independently of the experimental technique used (Figure 10a, ○, and Figure 10b). The temperature at the three-phase equilibrium is also lowered (by ca. 3 °C), although in a different manner, depending on the initial PVME concentration.[89] This probably relates to the fact that the invariant three-phase equilibrium at constant temperature, occurring in the strictly binary system, needs to be treated as a three-phase region when a third component (e.g., NaCl) is added. Hence, the initial composition will determine at which temperature three phases coexist, in agreement with other experimental work.[43,91] Furthermore, the stepwise change in both ultrasonic signals (during phase separation) is affected as well, resembling the observations made for the PNIPAM/water system (Figure 7); i.e., the presence of salt causes a diminution of Δ ultrasonic velocity, whereas Δ ultrasonic attenuation becomes larger. Note that the concentration range studied by HR-US (Figure 10b, □ and —) is limited to solutions with less than 30 wt % PVME, since more concentrated solutions exhibit sedimentation, causing a simultaneous decrease in both the

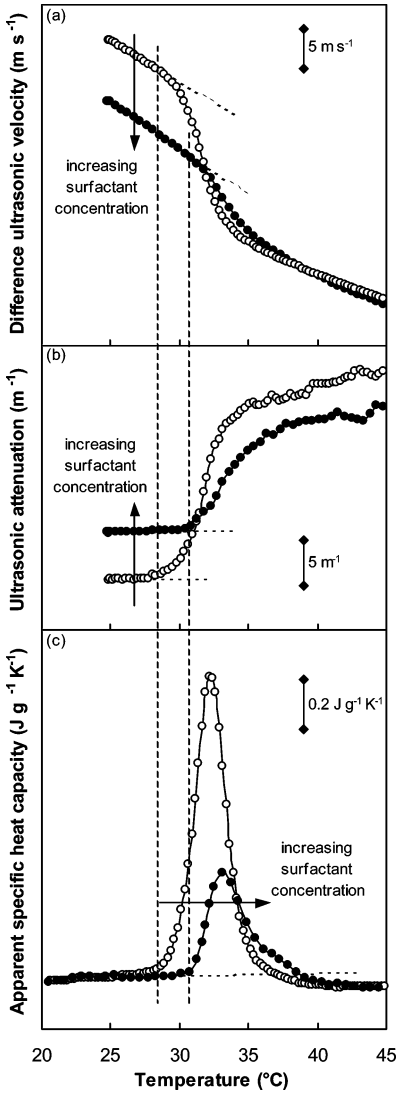

Figure 11. Nonisothermal demixing of 10/90 PNIPAM/water with varying amounts of SDS (0 and 0.035 M): (a) difference ultrasonic velocity, (b) ultrasonic attenuation, and (c) c_p^{app}. Lines are a guide to the eye.

velocity and the attenuation. This could not be avoided when stirring was applied.

Influence of Surfactant on the Phase Behavior of PNIPAM/Water. As already mentioned in the introductory part, surfactants are often used to stabilize aqueous dispersions of hydrophobic solutes. Therefore, the addition of surfactants will undoubtedly change the solution behavior of the polymers under investigation, which was previously thoroughly elaborated for dilute polymer solutions, usually using sodium dodecyl sulfate (SDS) as a surfactant.[63−67] These studies revealed that the SDS molecules adsorb onto the PNIPAM chains, which, due to electrostatic repulsion, consequently results in an increase of polymer dimensions.[68] Hence, the scattering ability of the supplementary swollen (entangled) PNIPAM coils will increase, causing a larger ultrasonic attenuation value in the homogeneous region (Figure 11b, compare ○ with ●). This observation holds for each composition. In contrast, the addition of salt hardly influences the ultrasonic attenuation below T_{demix} (Figure 6b), suggesting that both types of additives dissimilarly affect the polymer−water hydration structure. That is to say, salt ions primarily disrupt the configuration of water molecules, whereas the surfac-

tant used interacts with the polymer itself.

Nevertheless, the increased solubilization of the polymer chains causes an elevation of the phase separation temperature upon heating,[72−75] which nicely corresponds using either HR-US or MTDSC (Figure 11, vertical dashed lines). However, in contrast with the previously described salt effect, the (difference) ultrasonic velocity decreases when adding SDS, indicating a lower amount of bound water within the ternary mixture. As a result, the stepwise change in the difference ultrasonic velocity at T_{demix} becomes smaller, reflecting a reduced amount of released water molecules previously surrounding the PNIPAM chains. Hence, the endothermic heat effect from MTDSC is expected to become smaller, as confirmed in Figure 11c, since the demixing enthalpy describes the amount of hydrogen bonds broken. Note that the distribution of the heat effect in a reversing (i.e., c_p^{app}) and nonreversing contribution remains virtually unchanged; i.e., the largest part of the demixing enthalpy is still seen in the apparent specific heat capacity signal. Furthermore, the stepwise change in the ultrasonic attenuation, related to energy losses caused by aggregation, is at least halved, indicating a reduced level of chain association due to repulsive electrostatic interactions between the ionic heads of the adsorbed surfactant molecules.[76−79] These observations become less pronounced at higher polymer concentration, probably indicating that the amount of SDS added does not suffice to obtain a homogeneous distribution along the accessible polymer chains.

Conclusions

High-resolution ultrasonic spectroscopy (HR-US) and modulated temperature differential scanning calorimetry (MTDSC) have been successfully applied to study the influence of additives on the LCST phase behavior of aqueous polymer solutions for compositions spanning the entire concentration range. The evolution of both ultrasonic signals (i.e., velocity and attenuation, HR-US) as well as the apparent heat capacity signal (MTDSC) reflects the ongoing compositional changes with temperature, governed by the specific shape (type II or III) of the LCST demixing curve.

HR-US provides supplementary information (on a molecular level) concerning the solute−solute and water−solute interactions in the temperature region studied. The addition of salt generates a substantial increase of the ultrasonic velocity, signifying a considerable amplification of the amount of bound water. Moreover, the ultrasonic attenuation value in the homogeneous region remains unaffected, demonstrating that salt ions mainly modify the solvent properties. The resulting reduced polymer hydration structure increases the glass transition temperature of the homogeneous aqueous polymer solution, again illustrating the superior water-structuring capability of salt. Hence, the polymer−water interactions become partially disrupted, causing a decrease in demixing temperature both for aqueous solutions of PNIPAM or PVME. This effect becomes more pronounced at high polymer concentration, which results in an asymmetric shape of the LCST demixing curve. In addition, the amplified stepwise change in ultrasonic attenuation in the temperature range where compositional changes occur (heterogeneous region) reflects a larger degree of polymer aggregation.

The addition of a surfactant, on the other hand, results in an increase in demixing temperature together with a larger ultrasonic attenuation value in the homogeneous region and a smaller variation of both ultrasonic signals during phase separation. These observations result from the increased solubilization of the polymer chains, combined with electrostatic repulsions within the ternary mixture that limit the level of polymer association.

Acknowledgment. Kurt Van Durme thanks the Institute for the Promotion of Innovation through Science and Technology in Flanders (IWT) for a PhD scholarship. Prof. Vitaly Buckin from the Department of Chemistry at University College Dublin, Ireland, is acknowledged for fruitful discussions.

References and Notes

(1) Galaev, I. Y.; Mattiasson, B. *Tibtech* **1999**, *17*, 335−340.
(2) Kauzmann, W. *Nature (London)* **1987**, *325*, 763−764.
(3) Osada, Y.; Kishi, R.; Hasebe, M. *J. Polym. Sci., Part C: Polym. Lett.* **1987**, *25*, 481−485.
(4) Shinohara, S.; Tajima, N.; Yanagisawa, K. *J. Intell. Mater. Syst. Struct.* **1996**, *7*, 254−259.
(5) Liu, Z.; Calvert, P. *Adv. Mater.* **2000**, *12*, 288−291.
(6) Gotoh, T.; Okamoto, H.; Sakohara, S. *J. Chem. Eng. Jpn.* **2004**, *37*, 347−352.
(7) Rao, K. V. R.; Devi, K. P. *Int. J. Pharm.* **1988**, *48*, 1−13.
(8) Brazel, C. S.; Peppas, N. A. *Polym. Mater. Sci. Eng.* **1996**, *74*, 370−371.
(9) Qiu, Y.; Park, K. *Adv. Drug Del. Rev.* **2001**, *53*, 321−339.
(10) Gupta, P.; Vermani, K.; Garg, S. *Drugs Discov. Today* **2002**, *7*, 569−579.
(11) Kikuchi, A.; Okano, T. *Macromol. Symp.* **2004**, *205*, 217−227.
(12) Liang, L.; Rieke, P. C.; Liu, J.; Fryxell, G. E.; Young, J. S.; Engelhard, M. H.; Alford, K. L. *Langmuir* **2000**, *16*, 8016−8023.
(13) Choi, Y. J.; Yamaguchi, T.; Nakao, S. I. *Ind. Eng. Chem. Res.* **2000**, *39*, 2491−2495.
(14) Akashi, R.; Tsutsui, H.; Komura, R. *Adv. Mater.* **2002**, *14*, 1808−1811.
(15) Kanazawa, R.; Yoshida, T.; Gotoh, T.; Sakohara, S. *J. Chem. Eng. Jpn.* **2004**, *37*, 59−66.
(16) Miyata, T.; Uragami, T.; Nakamae, K. *Adv. Drug Del. Rev.* **2002**, *54*, 79−98.
(17) Schild, H. G. *Prog. Polym. Sci.* **1992**, *17*, 163−249.
(18) Maeda, H. *J. Polym. Sci., Part B: Polym. Phys.* **1994**, *32*, 91−97.
(19) Lin, S. Y.; Chen, K. S.; Run-Chu, L. *Polymer* **1999**, *40*, 2619−2624.
(20) Ramon, O.; Kesselman, E.; Berkovici, R.; Cohen, Y.; Paz, Y. *J. Polym. Sci., Part B: Polym. Phys.* **2001**, *39*, 1665−1677.
(21) Ohta, H.; Ando, I.; Fujishige, S.; Kubota, K. *J. Polym. Sci., Part B: Polym. Phys.* **1991**, *29*, 963−968.
(22) Maeda, Y. *Langmuir* **2001**, *17*, 1737−1742.
(23) Maeda, H. *J. Polym. Sci., Part B: Polym. Phys.* **1994**, *32*, 91−97.
(24) Boutris, C.; Chatzi, E. G.; Kiparissides, C. *Polymer* **1997**, *38*, 2567−2570.
(25) Van Durme, K.; Bernaerts, K. V.; Verdonck, B.; Du Prez, F. E.; Van Mele, B. *J. Polym. Sci., Part B: Polym. Phys.,* submitted for publication.
(26) Meeussen, F.; Nies, E.; Verbrugghe, S.; Goethals, E.; Du Prez, F. E.; Berghmans, H. *Polymer* **2000**, *41*, 8597−8602.
(27) Van Durme, K.; Verbrugghe, S.; Du Prez, F. E.; Van Mele, B. *Macromolecules* **2004**, *37*, 1054−1061.
(28) Afroze, F.; Nies, E.; Berghmans, H. *J. Mol. Struct.* **2000**, *554*, 55−68.
(29) Van Durme, K.; Van Assche, G.; Van Mele, B. *Macromolecules* **2004**, *37*, 9596−9605.
(30) Van Durme, K.; Loos, W.; Du Prez, F. E.; Van Mele, B. *Polymer* **2005**, *46*, 9851−9862.
(31) Meeussen, F.; Bauwens, Y.; Moerkerke, R.; Nies, E.; Berghmans, H. *Polymer* **2000**, *41*, 3737−3743.
(32) Swier, S.; Van Durme, K.; Van Mele, B. *J. Polym. Sci., Part B: Polym. Phys.* **2003**, *41*, 1824−1836.
(33) Šolc, K.; Dušek, K.; Koningsveld, R.; Berghmans, H. *Collect. Czech. Chem. Commun.* **1995**, *60*, 1661−1688.

(34) Schäfer-Soenen, H.; Moerkerke, R.; Berghmans, H.; Koningsveld, R.; Dušek, K.; Šolc, K. *Macromolecules* **1997**, *30*, 410−416.
(35) Nies, E.; Ramzi, A.; Berghmans, H.; Li, T.; Heenan, R. K.; King, S. M. *Macromolecules* **2005**, *38*, 915−924.
(36) Karlström, G. *J. Phys. Chem.* **1984**, *89*, 4962−4964.
(37) Qian, C.; Mumby, S. J.; Eichinger, B. E. *J. Polym. Sci., Part B: Polym. Phys.* **1991,** *29*, 635−637.
(38) Qian, C.; Mumby, S. J.; Eichinger, B. E. *Macromolecules* **1991**, *24*, 1655−1661.
(39) Horst, R. *J.* Phys. *Chem. B* **1998** *102*, 3243−3248.
(40) Wolf, B. A. *Macromolecules* **2005**, *38*, 1378−1384.
(41) Kenkare, P. U.; Hall, C. K. *AIChE J* **1996**, *42*, 3508−3522.
(42) Pessôa Filho, P. A.; Mohamed, R. S. *Braz. J. Chem. Eng.* **2001**, *18*, 449−458.
(43) Bergé, B.; Koningsveld, R.; Berghmans, H. *Macromolecules* **2004**, *37*, 8082−8090.
(44) Koningsveld, R.; Stockmayer, W. H.; Nies, E. *Polymer Phase Diagrams*; Oxford University Press: Oxford, England, 2001.
(45) Wertheim, M. S. *J. Stat.* Phys. **1984,** *35* 19−34.
(46) Van Durme, K.; Loozen, E.; Nies, E.; Van Mele, B. *Macromolecules*, in press.
(47) Loozen, E.; Van Durme, K.; Van Mele, B.; Berghmans, H.; Nies, E. *Polymer*, submitted for publication.
(48) Van Durme, K.; Van Assche, G.; Nies, E.; Van Mele, B. *Macromolecules*, in press.
(49) Horne, R. A.; Almeida, P.; Day, A. F.; Yu, N. T. *J. Colloid. Interface Sci.* **1971**, *35*, 77−84.
(50) Ataman, M.; Boucher, E. A. *J. Polym. Sci., Polym. Phys. Ed.* **1982**, *20*, 1585−1592.
(51) Nwankwo, I.; Xia, D. W.; Smid, J. *J. Polym. Sci., Part B: Polym. Phys.* **1988**, *26*, 581−594.
(52) Pang, P.; Englezos, P. *Fluid Phase Equilib.* **2002**, *194−197*, 1059−1066.
(53) Schild, H. G.; Tirrell, D. A. *J. Phys. Chem.* **1990**, *94*, 4352−4356.
(54) Yang, Y.; Zeng, F.; Tong, Z.; Liu, X.; Wu, S. *J. Polym. Sci., Part B: Polym. Phys.* **2001**, *39*, 901−907.
(55) Brackman, J. C.; Engberts, J. B. F. N. *Langmuir* **1991**, *7*, 2097−2102.
(56) Mikheeva, L. M.; Grinberg, N. V.; Mashkevich, A. Y.; Grinberg, V. Y.; Thanh, L. T. M.; Makhaeva, E. E.; Khokhlov, A. R. *Macromolecules* **1997**, *30*, 2693−2699.
(57) Baltes, T.; Garret-Flaudy, F.; Freitag, R. *J. Polym. Sci., Part A: Polym. Chem.* **1999**, *37*, 2977−2989.
(58) Kirsh, Y. E.; Yanul, N. A.; Popkov, Y. M. *Eur. Polym. J.* **2002**, *38*, 403−406.
(59) Hofmeister, F. *Arch. Exp. Pathol. Pharmakol.* **1888**, *24*, 246−260.
(60) Collins, K. D. *Biophys. J.* **1997**, *72*, 65−76.
(61) Omta, A. W.; Kropman, M. F.; Woutersen, S.; Bakker, H. J. *J. Chem. Phys.* **2003**, *119*, 12457−12461.
(62) Terayama, H.; Hirota, K.; Yoshimura, T.; Esumi, K. *Colloids Surf. B* **2002**, *27*, 177−180.
(63) Tam, K. C.; Wu, X. Y.; Pelton, R. H. *J. Polym. Sci., Part A: Polym. Chem.* **1993**, *31*, 963−969.
(64) Tiktopulo, E. I.; Uversky, V. N.; Lushchik, V. B.; Klenin, S. I.; Bychkova, V. E.; Ptitsyn, O. B. *Macromolecules* **1995**, *28*, 7519−7524.
(65) Faes, H.; De Schryver, F. C.; Sein, A.; Bijma, K.; Kevelam, J.; Engberts, J. B. F. N. *Macromolecules* **1996**, *29*, 3875−3880.
(66) Zhu, P. W.; Napper, D. H. *Phys. Rev. E* **2000**, *61*, 6866−6871.
(67) Hai, M.; Han, B.; Yan, H. *J. Phys. Chem. B* **2001**, *150*, 4824−4826.
(68) Peng, S.; Wu, C. *Macromolecules* **2001**, *34*, 568−571.
(69) Mears, S. J.; Deng, Y.; Cosgrove, T.; Pelton, R. *Langmuir* **1997**, *13*, 1901−1906.
(70) Mylonas, Y.; Staikos, G.; Lianos, P. *Langmuir* **1999**, *15*, 7172−7175.
(71) Abuin, E.; Leon, A.; Lissi, E.; Varas, J. M. *Colloids Surf. A* **1999**, *147*, 55−65.
(72) Ricka, J.; Meewes, M.; Nyffenegger, R.; Binkert, T. *Phys. Rev. Lett.* **1990**, *65*, 657−660.
(73) Wu, C.; Zhou, S. *J. Polym. Sci., Part B: Polym. Phys.* **1996**, *34*, 1597−1604.
(74) Kunugi, S.; Yamazaki, Y.; Takano, K.; Tanaka, N.; Akashi, M. *Langmuir* **1999**, *15*, 4056−4061.
(75) Jean, B.; Lee, L. T.; Cabane, B. *Colloid Polym. Sci.* **2000**, *278*, 764−770.
(76) Makhaeva, E. E.; Tenhu, H.; Khokhlov, A. R. *Macromolecules* **1998**, *31*, 6112−6118.
(77) Gao, Y.; Au-Yeung, S. C. F.; Wu, C. *Macromolecules* **1999**, *32*, 3674−3677.
(78) Lee, L. T.; Cabane, B. *Macromolecules* **1997**, *30*, 6559−6566.
(79) Ando, M.; Takahashi, D.; Takeda, S.; Nakajima, H. *Jpn. J. Appl.* Phys. **1997**, *36*, 2955−2958.
(80) Buckin, V.; Smith, C. *Semin. Food Anal.* **1999**, *4*, 113−127.
(81) O'Driscoll, B.; Smyth, C.; Alting, A. C.; Visschers, R. W.; Buckin, V. *Spectrosc. Eur.* **2003**, *15*, 20−25.
(82) Buckin, V.; Kudryashov, E.; O'Driscoll, B. *Pharm. Tech. Eur.* **2002**, *14*, 33−37.
(83) Van Durme, K.; Delellio, L.; Kudryashov, E.; Buckin, V.; Van Mele, B. *J. Polym. Sci., Part B: Polym. Phys.* **2005**, *43*, 1283−1295.
(84) Van Durme, K.; Rahier, H.; Van Mele, B. *Thermochim. Acta*, submitted for publication.
(85) Kudryashov, E.; Kapustina, T.; Morrissey, S.; Buckin, V.; Dawson,K. *J. Colloid Interface Sci.* **1998**, *203*, 59−68.
(86) Smyth, C.; Kudryashov, E.; Buckin, V. *Colloids Surf. A* **2001**, *183−185*, 517−526.
(87) Xu, Y.; Li, L. *Polymer* **2005**, *46*, 7410−7417.
(88) Kesselman, E.; Ramon, O.; Berkovici, R.; Paz, Y. *Polym. Adv. Technol.* **2002**, *13*, 982−991.
(89) Maeda, Y.; Nakamura, T.; Ikeda, I. *Macromolecules* **2001**, *34*, 1391−1399.
(90) Buckin, V.; Kankiya, B. I.; Kazaryan, R. L. *Biophys. Chem.* **1989**, *34*, 211−223.
(91) Meeussen, F. Ph.D. Thesis, Catholic University of Leuven, 2002.

MA051816T